Chapter 5

Discussion

5.1 Modeling Technique

5.1.1 On What Projects is Theory Likely to Have an Impact?

Computational chemistry can today be applied to any problem involving common elements and an arbitrary amount of data can be produced. But research campaigns should be directed by the pressing needs of industry or the public, or by curiosity, not by the likelihood of producing a paper using a certain set of tools. The goal of asking this question is then identifying to which of the many catalysis projects worthy of attention is theory likely to contribute consequential new insights or design principles.

Since computational techniques are not yet capable of predicting all the relative rates connecting all the intermediates one can hypothesize for a reaction network, at least some experimental observations of reactions related to the goal must be present. A new catalytic cycle could be proposed from scratch, but analyzing each step for thermodynamic feasibility and selectivity would be prohibitively time-consuming with the current state of the art (not to mention issues of accuracy). Observations of known reactions, if only qualitative, can quickly point to the step in a cycle that needs improvement. For example, upon reacting some catalyst formulation and a substrate, are no products observed, or stoichiometric amounts? Or catalytic amounts mixed with some unwanted byproduct? Or a decomposed catalyst? Quantitative measurements, which alone may not explain *why* a reaction shows low rates or selectivity or fails to run in some solvent, can go one step further by verifying a model that does offer an explanation. A research topic should include well-defined goals that are still unreached, so that any new insights from theory will have an opportunity to lead back to useful developments rather than remain interesting but idle. Such goals also help keep attention focused on the reaction steps that *need* to be understood. Also, the size of the model that is necessary to capture the relevant geometric and chemical properties of the system (which are at first unknown) must be manageably small. Faster computers and the methodological developments mentioned in Chapter 1 have not yet obviated this concern. Since wavefunctions and costly derivatives of the total energy will inevitably be calculated time and time again, care must be taken to identify how much of a catalyst must be represented in the model. In the case of hierarchical approaches this includes identifying what may be treated with higher or lower levels of theory. (Should bulky side chains on a ligand or distant amino acids in a protein be treated quantum mechanically or with a forcefield? Should solvent molecules be included excplicitly?) While studying hydrodesulfurization reactions over MoS_2 crystals, it was found that models had to contain about six (MoS_2) units to faithfully reproduce the structure of bulk molybdenite and not relax into amorphous aggregations. Simply converging wavefunctions for these models and their large organic adsorbates proved to be a severe bottleneck to understanding the trends observed in that family of reactions. Paring away physical phenomena or atoms that may not be essential in order to make more tractable models can lead to the unproductive cycle of modifying models until they reproduce experimental observations.

Modeling heterogeneous and homogeneous processes both raise specific difficulties, though both fields contain reactions which are important enough to for us to overcome those difficulties. Studying reactions on solids is uniquely complicated by surfaces' likelihood to differ from a clean termination of a bulk crystal structure (when a periodic structure is even present) and to vary with time and conditions. X-ray structures of homogeneous complexes, while they may not represent the *in situ* state of the complex, limit the number of likely formulations of the catalyst's resting state, and organic ligands rarely decompose on the time scale of the reactions they promote. Determining the definition of active sites on a surface can be as difficult as determining the mechanism of the reaction in question and is prerequisite to computing activation energies and understanding poisoning. Capturing the electronic structure of a quasi-infinite crystal in a tractable model is another challenge being addressed by both finite cluster models and periodic models. Metals can interact with species adsorbed on their surface as a compensating dielectric medium and as a reservoir of electronic charge and spin. Understanding the electron distribution of the bare surface can help find the smallest model capable of describing surface-adsorbate bonding and charge transfer (see [88] for example). Since models of solids are likely to include many atoms not directly involved in the reaction and complex metallic or semiconducting wavefuntions, valuable time can be spent simply nudging wavefunctions toward convergence. Finally, a library of organic syntheses exists to help us implement new design elements into ligands for homogeneous catalysts, but the degrees of freedom available when synthesizing a new surface (composition, dopants, preparation) are ultimately susceptible to the will of thermodynamics through annealing. Standing in favor of heterogeneous studies is our ability to accurately calculate thermodynamics and geometries for solid and gas phase species, while predicting entropies in the liquid phase remains a challenge.

5.1.2 What to Do and Not to Do

The decades since quantum mechanics was first applied to atoms and molecules have produced introductory texts and advanced literature on the physical interpretation and mathematical implementation of the ever evolving methods in quantum chemistry. The use of quantum mechanics to find solutions to real chemical problems, however, has not matured to the point of being codified. Some of the guidelines that have become apparent so far are discussed here.

Many corollaries, and some of the strategies below, flow from a central idea, or "First Law of Computational Catalysis": **In experiments you see what thermodynamics allows, not necessarily what you want. In calculations, you see what you want, not necessarily what thermodynamics allows.** Apparent in this are a key strength (the ability to pause a reaction at any point or study scenarios that are unlikely or impossible) and weakness (models must be validated) of simulations.

Do test the thermodynamics, geometries, or other quantities predicted by your method against known experimental values for small molecules containing the relevant elements. Pseudopotentials, basis sets, density functionals and other approximations tend to fail under certain conditions. Identifying and correcting such failures is of course best done before an investigation is underway. After the proterties of gas phase species have been validated, solution phase experimental data may be used to test solvation models, if such data is available.

For example, when studying redox reactions between gold complexes and sulfur species, the popular 6-31G**++ [23] basis set and others were found to be incapable of accurately describing the thermodynamics of sulfur species across the range of oxidation states. The illustrative results in Table 5.1 show that error tends to increase as the difference between the reactant's and product's oxidation state increases, with the calculations destabilizing higher oxidation states.

Table 5.1: Thermodynamics of sulfur reductions predicted with several basis sets

Basis set (sulfur[1])	Nr. of basis functions on S	ΔH^{298K} (kcal/mol) $SO_3(g) + CH_4(g) \rightarrow SO_2(g) + CH_3OH(g)$	 $SO_3(g) + 4H_2(g) \rightarrow H_2S(g) + 3H_2O(g)$
Experimental		-6.7	-83.7
lav3p**++[2]	9	-54.6	-194.4
6-31G**++	22	-21.7	-117.3
cc-PVTZ(-F)++[3]	36	-17.1	-105.0
6-31G augmented[4]	27	-12.9	-94.3

[1] All atoms other than sulfur use 6-31G**++ in all cases. [2] Reference [41] [3] Reference [89] [4] Described in text

Martin [90] addressed this problem and found that in order for polar bonds to be well described, sulfur (and likely the other elements in its row) requires a basis set which includes d-type functions properly sized to polarize the 2p core orbitals (in addition to the diffuse d-functions commonly used to polarize the 3p valence functions). Martin, using coupled cluster (CCSD(T)) calculations, found that as the basis set was expanded, the bond dissociation energy and geometry of SO_2 approached and matched the experimental values. As a more practical solution, we replaced the single polarization shell of the 6-31G**++ basis with just two d-functions, which were optimized to minimize the energy of SO_3. The exponent of the diffuse polarization function was adjusted from $\alpha = 0.65$ (in the Pople basis) to $\alpha = 0.55$ and the new, tight d-shell was a contraction of two Guassians with exponents $\alpha_1 = 7.5$ and $\alpha_2 = 1.8$ with contraction coefficients $c_1 = 0.2$ and $c_2 = 1.0$. This augmented basis set provides a better description than the many valence functions of the cc-PVTZ(-F)++ basis, and the error that remains is systematic with the oxidation state of sulfur.

Do identify the resting state of the catalyst before beginning mechanistic investigations. This aids in writing rate laws and identifying modes of ground state stabilization that can poison a catalyst. Solvent molecules, driven by their concentration, can replace ligands on metal complexes in solution, and solid surfaces are known to undergo crucial reconstructions to minimize their free energy. Activation energies calculated using the wrong ground state will not match observed barriers even if the rate-limiting transition state is being modeled correctly. Scheffler, et al., ([91] and references within) have demonstrated the identification of the stable reconstructions of surfaces as a function of conditions from first principles using DFT and Monte Carlo techniques.

Do try to locate side reactions that could kill a catalytic cycle if the cycle has not been experimentally demonstrated. Often we try to manipulate a structure so that a reaction step has a low barrier or becomes exothermic. When a satisfying structure is found we should suspect that it is simply unstable and check for decomposition pathways. Unrealistic species high on the potential energy surface may appear misleadingly reactive and are irrelevant.

For example, 2,2'-biimidazolylidene (bmdz, Figure 5.1) had been suggested as a promising ligand for platinum-catalyzed methane activation in sulfuric acid. The activation barrier for cleaving the C-H bond of methane with a (bmdz)Pt^{II} complex had been predicted to be low by analogy to the (experimentally proved [92]) (2,2'-bipyrimidine)$PtCl_2$ catalyst. However, before effort was invested in the synthesis of (bmdz)Pt complexes, we found that the bmdz ligand was unstable with respect to reduction by any number of species present in the reaction mixture. The π-system of biimidazolylidene contains only ten electrons, so the driving force to oxidize two electrons from a donor and become 2,2'-biimidazole (biim, with twelve aromatic electrons) is strong. For instance, (bmdz)$Pt(OSO_3H)_2$ is predicted to react exothermically with two molecules of H_2SO_4 to form the Pt^{IV} complex (biim)$Pt(OSO_3H)_4$. This intermediate can then be passivated by methane to produce one molecule of methyl bisulfate and the Pt^{II} complex (biim)$Pt(OSO_3H)_2$. This complex might also be active for methane oxidation, except that the neutral biimidazole ligand is basic enough to be protonated off platinum to form, for example, (η^1-biimH^+)$Pt(OSO_3H)_3$. Four inequivalent doublets in ^{1}H-NMR spectra and crystal structures of related compounds[93] suggest the biim ligand is monodentate in solution instead of chelated as desired.

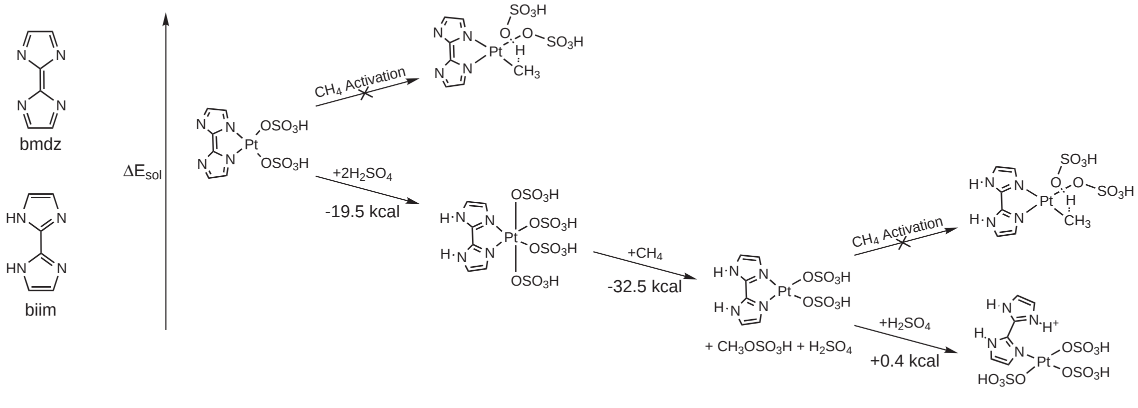

Figure 5.1: Deactivation pathways of 2,2'-biimidazolylidene and 2,2'-biimidazole-based platinum catalysts.

On the other hand, **do model what is unlikely or impossible in order to understand why.** Even if a reaction is known to follow mechanism A, simulating mechanism B can offer more explanation for why A is favored, as well as suggest why changes to the reaction's participants might cause mechanism B to become favored. Also, a useful decomposition of bond strengths is found by first separating the two fragments (perhaps a ligand and metal complex) with their atomic coordinates *frozen* (giving the "electronic" bond strength), then allowing the separate fragments to relax (yielding the geometric strain energy incurred upon bonding).

For example, periodic DFT calculations[1] were performed to identify the major factors determining a transition metal disufide's (TMS) crystal structure. As seen in Table 5.2, most TMS adopt one of four structure types: CdI_2 ($P\overline{3}m1$), molybdenite (P63/mmc), pyrite (Pa3), and marcasite (Pnnm). The former two feature loosely stacked layers while the latter are covalently bound in every direction. In the molybdenite structure the metal atoms are coordinated as trigonal prisms, while in the other three structures the metals are octahedrally coordinated. A second distinguishing factor is the environment of sulfur atoms. Sulfur atoms in CdI_2 and molybdenite materials are bound to three metal atoms, and have their nearest sulfur neighbors either across the slab (about

---

[1] Periodic density functional calculations were performed with the Cambridge Serial Total Energy Package[94], using the gradient-corrected functional of Perdew and Wang. Default pseudopotentials were used with band-by-band minimization of the total energy by variation of the plane-wave expansion coefficients. Cutoff energies for plane waves were 500 or 600 eV, and finite basis set corrections were used.

3 Å away) or in adjacent slabs (about 4 Å away). In pyrite and marcasite materials, on the other hand, sulfur atoms are found in covalently bonded pairs, leaving them tetrahedrally coordinated to three metal atoms and one sulfur atom.

Table 5.2: Observed disulfide crystal structures (from [95])

Ti	V		Mn	Fe	Co	Ni	Cu	Zn
CdI_2	CdI_2		Pyr	Pyr/Mar	Pyr	Pyr	Pyr	Pyr
Zr	Nb	Mo		Ru	Rh	Pd		Cd
CdI_2	Mol[1]	Mol[1]		Pyr	Pyr	PdS_2		Pyr[2]
Hf	Ta	W	Re	Os	Ir	Pt		
CdI_2	CdI_2[1]/Mol	Mol	Mol	Pyr	Pyr	CdI_2		

[1] Alternate stacking sequence [2] Observed under high pressure

For the calculations, metals were chosen to represent the four structure types and the breadth of the transition series. For each of the metals, four unit cells were constructed; one with the symmetry of the naturally occurring disulfide of that metal, and three with the symmetries of the other three structure types. All of these unit cells were relaxed, keeping the symmetry intact but allowing cell dimensions and atomic positions to settle to their lowest-energy values. The resulting set of structures could then be compared to determine the energy cost for a particular TMS to adopt one of its virtual structures and whether any of these virtual phases is particularly low-lying in energy. In addition, how each metal adapts the foreign structure types to arrive at local energy minima was observed. The energies of all phases calculated, shown in Table 5.3 relative to the lowest energy phase for each metal, show that CASTEP generally predicted the naturally occurring structures to have the lowest energy.

Periodic trends in the TMS structures predicted by CASTEP suggest a relation between a metal's ability to donate electrons to sulfur and the structure type preferred by the metal. For example, take the molybdenite structures predicted for each metal considered. The distance between the eclipsed sulfur atoms in each layer decreases as the metal is varied from left to right across the periodic table (Figure 5.2). In the case of MoS_2(mol), presumably the sulfur atoms get enough charge from their bonds to the Mo atoms that they do not need to form sulfur-sulfur bonds. On the other hand,

Table 5.3: Relative energies of relaxed disulfide structures (eV/metal atom).

Metal	Structure Type			
	CdI_2	Molybdenite	Pyrite	Marcasite
Zr	**0.0**[1]	0.3	0.6	0.3
Ti	**0.0**	0.2	0.8	0.4
Mo	1.0	**0.0**	1.8	0.9
Ru	1.7	1.9	**0.0**	0.1
Fe	1.3	1.7	0.0	**0.0**
Ni	0.3	0.7	**0.1**	0.0
Cd	2.4	1.5	**0.3**	0.0

[1] Bold denotes a metal's experimentally observed structure type.

the sulfurs in CdS_2(mol) pull toward each other across the slab, apparently to increase the charge available to each.[2] On the left side of the Periodic Table, the preferred S-S distance is compatible with the geometry inherent to the molybdenite structure type. That is, a 3.1 Å S-S distance results in an S-Mo-S angle of about 80°, which is natural for a trigonal prismatically coordinated metal atom. The 2.25 Å S-S distance adopted by CdS_2(mol) requires S-Cd-S angles of 50°, which no doubt involve significant strain energy. Since the tendency of CdS_2 to form S-S bonds and the tendency of trigonal prismatically coordinated metals to form wider bond angles are at odds in the molybdenite structure, CdS_2(mol) is a relatively high energy phase and CdS_2 adopts a different structure. And so with the other late transition metals.

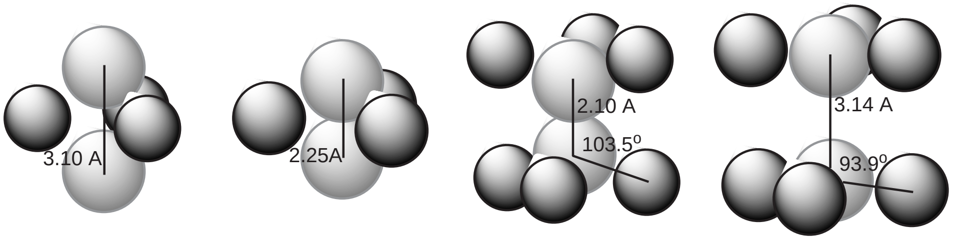

MoS_2(mol) CdS_2(mol) RuS_2(pyr) ZrS_2(pyr)

Figure 5.2: Sulfur-sulfur bonding in transition metal disulfides. Metal atoms dark, sulfur atoms light.

The late transition metal disulfides adopt the pyrite and marcasite structures, in which the coordination of atoms naturally includes S-S bonding. When a more easily oxidized metal such as zirconium adopts such a structure, the CASTEP results show that the sulfur atoms are pushed away from each other (3.14 Å). As the S-S distance increases, the tetrahedral coordination of sulfur

---

[2] The CdI_2 structures of later transition metals draw sulfurs together by decreasing the distance between layers.

becomes triangular, presumably at a cost in energy. This trend is evident as the S-S-M bond angle in the pyritic structures expands from nearly perpendicular at the beginning of the transition metals (94° in ZrS_2(pyr)) to nearly tetrahedral by the end (104° in RuS_2(pyr)). So the early transition metal disulfides, whose sulfur atoms do not benefit from S-S bonding, adopt the CdI_2 and molybdenite structure types. The early TMS structures can then be labeled $M^{IV}(S^{-2})_2$ and the late ones $M^{II}(S_2)^{-2}$.

Regarding the choice of early transition metals between the CdI_2 and molybdenite structures, one recalls the difference in the coordination of metal atoms in the two layered structures and suggests that the choice is based on the metals' preference for trigonal prismatic or octahedral coordination. This preference, stemming from the electronic configuration of the metal, was demonstrated by a few finite cluster calculations with Mo and Zr. Geometry optimizations were performed on four clusters: MoS_6 and ZrS_6, each in octahedral and trigonal prismatic coordination. The MoS_6 cluster preferred the trigonal prismatic coordination (with eclipsed S-Mo-S bond angles of 79.7°) to the octahedral coordination by 13 kcal/mol. On the other hand, the ZrS_6 cluster preferred the octahedral coordination to the trigonal prismatic coordination (with eclipsed S-Zr-S bond angles of 78.0°) by 30 kcal/mol[3]. Zr^{IV} is left with no d electrons, so the most stable arrangement of six bonds to sulfurs is octahedral. Mo^{IV} retains a pair of d electrons, and these prefer to occupy the non-degenerate a_1' orbital of the D_{3h} coordination over breaking the degeneracy of the t_{2g} group of octahedral coordination.

Do hypothesize and discount as many mechanisms as possible when proposing a mechanistic explanation for an observed reaction. Underlying many unconvincing theory papers is the argument, "This is the mechanism we have described computationally, therefore it is the relevant mechanism" instead of, "The mechanism we have described is corroborated by observations while other plausible mechanisms are not." Experimental data in the form of reaction orders, rates, or chemo- or stereoselectivities is ideal for distinguishing among competing mechanisms (see section 4.2.1). Often discounting a mechanism is as easy as showing one intermediate to be thermodynam-

---

[3] Both octahedra were constrained only to D_{3d} symmetry but relaxed to nearly perfect octahedra.

ically inaccessible from the reactant state. The process of imagining new pathways (or comparing the different permutations of a series of elementary steps) can identify routes which offer clearer explanations for observed phenomena than what had previously been suggested. The routes by which bonds are broken and formed in real reactions no doubt extend beyond those that have yet been canonized in inorganic chemistry texts.

Complementary to discounting pathways, one should demonstrate as much quantitative agreement as possible between experiment and a suggested mechanism. However, the goal of simulations is not to develop a model until it reproduces experimental measurements. After a model has been validated, it must yield explanations for the measurements that would not be available otherwise. The computational description of a reaction should also be applied to new, related reactions or catalysts which have not been studied experimentally.

When hypothesizing and screening new ligands, **do base designs on structural motifs for which syntheses are known.** This will increase the probability of someone agreeing to and succeeding in synthesizing and testing it. The inclusion of rare heteroatoms, sensitive functional groups, multiple stereocenters, etc., may allow a designed molecule to perform wonderfully in the computer, but ultimately the merit of the design must also be based on its feasibility. Modern databases of known chemical compounds include enough structures that this constraint can be met with considerable freedom remaining.

5.2 Future Work

Increasing the potency of theoretical approaches in inorganic chemistry requires continued expansion of the kinds of quantities which can be predicted and the speed and accuracy of the predictions. New techniques will allow models to incorporate more of the environment which hosts reactions, quantitatively treat thermal and optical excitations and electron transfer events which can initiate reactions, and allow wider comparison between predicted and experimental nuclear, electronic and IR spectroscopic results. Methods mentioned here are not the sum of what is being developed in labs around the world; they are only the tools which will aid efforts to design catalysts most.

The most important technique still being developed is the ability to calculate accurate (and separate) enthalpy and entropy changes for general reactions in solution. Extending electronic energies to measureable properties of gas phase or surface-bound species can be done with useful accuracy through analytical formulas of statistical mechanics, but partition functions of solution phase and enzymatic moieties are affected by atoms not contained in the quantum mechanical model. Not all reactions allow the delegation of different contributions to the thermodynamic properties (e.g., solute-solvent electrostatic interactions, internal vibrational energy, configurational entropy, etc.) to different computational methods (e.g., polarizable continuum models, normal mode analysis, statistical mechanics, etc.). Solvent molecules not only affect the minimum-energy structure of a solute, but also the dynamics of the solute around that minimum by constraining its translation, rotation and conformational freedom. The contribution of the solute's six external degrees of freedom to entropy are a recurring difficulty when modeling solvated species, and the continuum solvent models do not address the issue. For unimolecular reactions $A \rightarrow B$, these elusive quantities cancel to a useful approximation, but for as simple a process as a catalyst binding a substrate, they can prevent the comparison of simulations and measured equilibrium constants or activation parameters. By employing a macroscopic dielectric constant, polarizable continuum models effectively capture both the electrostatic interactions (energy stabilization) of solute and solvent and the reorganization (entropy penalty) of solvent molecules near a non-uniform charge distribution. Unfortunately, the free energy of solvation that results from these models is not separable into its enthalpic and entropic components. In many cases (low dielectric media or neutral species in high dielectric media) the $-T\Delta S$ component of the solvation free energy is negligible and enthalpy can be calculated as in Equation 1.1. Table 5.4 illustrates, however, that when the magnitude of charges on species changes during a reaction, the free energy change, but not ΔH or ΔS, can be predicted. (And this much only in the case that librational entropy can be handled with the same accuracy. In table 5.4 the rotational and translational entropies of species with similar heavy atom were assumed to cancel, and experimental total entropies were used for H_2O(aq) and Cl^-(aq)[4].)

---

[4] The absolute entropy of Cl^-(aq) was obtained assuming the absolute entropy of H^+(aq) to be -21 J/mol·K [96].

Table 5.4: Calculated and experimental enthalpies and free energies of solution-phase reactions.

Reaction		ΔG° (kcal/mol)		ΔH° (kcal/mol)	
		Calc	Exp	Calc	Exp
$HSO_4^-(aq) + H_2O(aq)$	$\rightarrow SO_4^{2-}(aq) + H_3O^+(aq)$	3.9	2.7	2.8	-5.2
$HSeO_4^-(aq) + H_2O(aq)$	$\rightarrow SeO_4^{2-}(aq) + H_3O^+(aq)$	3.2	2.6	2.2	-4.2
$HSO_3^-(aq) + H_2O(aq)$	$\rightarrow SO_3^{2-}(aq) + H_3O^+(aq)$	9.5	9.9	8.5	-2.2
$PdCl_4^{2-}(aq) + 3H_2O(aq)$	$\rightarrow PdCl(H_2O)_3^+(aq) + 3Cl^-(aq)$	9.0	11.0	11.8	2.6

Within the polarizable continuum model there are areas which further research may improve. In addition to the electrostatic interactions of solute and solvent, continuum models often add a "cavity" term to describe the free energy cost of creating a solute-shaped vacuum in the solvent. This contribution has been parameterized using small hydrocarbons in water[97], but is not known in general. Only a few kcal/mol in magnitude, it is dominated by the electrostatic factors in many cases, but may be important in determining small energy differences, e.g., between regioselective transition states.

The locations of point charges representing the solvent are chosen around the solute using predefined atomic radii. For the most common elements, these radii have been optimized to reproduce known solvation energies, and in some cases are defined for specific hybridizations or functional groups. For most of the periodic table, however, radii are taken somewhat arbitrarily from tabulations of van der Waals radii. Even optimal static radii cannot accurately describe the spatial extent of elements whose oxidation state (and therefore size) may vary widely as in metals or hypervalent main group elements. Since the results of the solvation routine are sensitive to the radii employed (strongly sensitive in the case of charged particles), the current situation leaves one wanting a method in which the solute-solvent interface is based on first principles and is sensitive to the electronic characteristics of the given solute. It may be that the most useful interface, to which the current static atomic radii are a good approximation, is in general a function of the solute's gas phase electron density. Since this density is known at the time of a solvation calculation, it could easily furnish an iso-density surface, or a surface outside which a certain amount of electron density lies, if such a surface were shown to accurately represent the solvent-accessible surface of the solute.

Knowledge of dielectric constants' temperature dependence may furnish a means of discerning the enthalpic and entropic components of the solvent's reaction to a solute. Many other aspects of continuum solvation models are reviewed in [98]. If we desire, however, a method which describes the solute's external degrees of freedom and their explicit interaction with solvent molecules, we should begin to consider incorporating explicit molecular dynamics (MD) simulations into our protocol. The use of MD to provide partition functions will not be reviewed here, but note that we may benefit, depending on our approach, from not concerning ourselves with the general problem of computing total entropies and enthalpies with only a forcefield. First, the long simulation times required to sample enough configurations of the bulk solvent to enable absolute entropy estimations may not be necessary when solvent-solvent components of the total Hamiltonian can be separated from solvent-solute or solute-solute components[99]. Second, since the energy changes associated with bond energies would still be provided by quantum mechanics (QM), the forcefield employed would only have to treat intermolecular forces and vibrational frequencies accurately. (It would not require the complexity or extensive training set of a reactive forcefield.)

For the general solution-phase reaction $\mathsf{A} \rightarrow \mathsf{B} + \mathsf{C}$ we can illustrate three thermodynamic cycles that might be used incorporating properties calculated with MD (Figure 5.3). First consider an approach in which the solute's internal degrees of freedom are treated quantum-mechanically as usual while molecular dynamics are performed on a periodic box of solvent molecules and a solute molecule treated as a rigid body. All internal energy and enthalpy components, as well as the reorganization entropy of the solvent, could be computed using DFT (including a normal mode analysis of the QM-derived Hessian) and the polarizable continuum solvent model. Only the enthalpy and entropy of the solutes' external degrees of freedom would be provided by analysis of the classical trajectory[100]. The advantages of isolating the external modes of the (rigid) solute for classical treatment are: the forcefield could remain ignorant of the intricacies of metal-ligand bonds found in catalytic species, the solute's high-frequency vibrations would be accurately evaluated and their excitations treated with the correct statistics (whereas a classical treatment "excites" all modes, even below their characteristic temperatures), and transition state structures located with QM would not "fall" down to products or reactants during the dynamics.

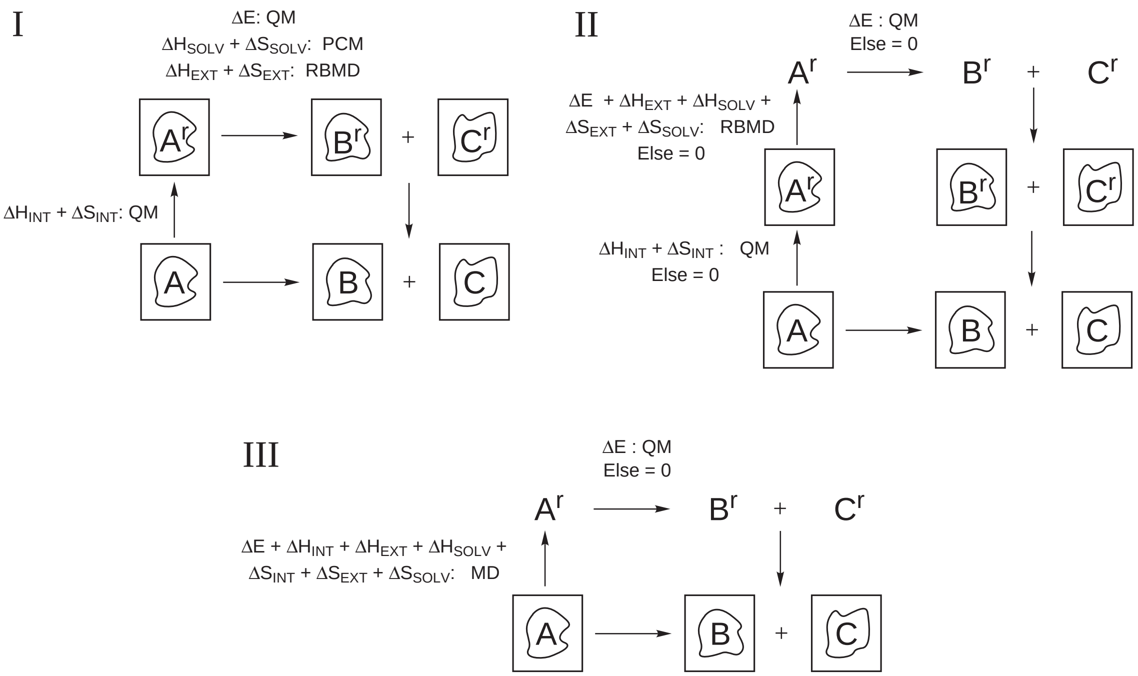

Figure 5.3: Possible thermodynamic cycles incorporating information from MD and QM to account for the various contributions to the total free energy change. Boxes denote solvated species (either explicitly or by continuum), superscript r denotes a (rigid) body with no internal motion, PCM = polarizable continuum method, RBMD = rigid body MD, INT/EXT = corresponding to internal/external degrees of freedom, SOLV = corresponding to solute-solvent and solvent-solvent interactions.

This method includes several shortcomings. Currently, calculation of the $(3N)^2$ Hessian elements becomes prohibitively slow for the large (100 atom) molecules for which geometry optimizations are now routine. Of more concern are the assumptions, the latter implied by the absence of explicit solvent molecules during the Hessian calculation, that the solute's low frequency vibrational modes are (1) harmonic and (2) not affected by the surrounding solvent. Consider the lowest-frequency modes (below 50 cm^{-1}) computed in the gas phase for the palladium complex in Figure 5.4. Treated as independent quantum mechanical harmonic oscillators[5], these modes (unhindered in the gas phase) contribute 73 cal/mol·K to the internal entropy. To estimate the effect of solvent molecules crowded around this solute, assume the effective frequencies of these twelve modes were collectively shifted up to 50 cm^{-1}, roughly the frequency at which molecules vibrate in liquid benzene. Now these modes would contribute 58 cal/mol·K. 15 cal/mol·K error is the same order of magnitude

---

[5] Even in vacuum, treating such modes, which include low-barrier rotations, as harmonic oscillators may lead to considerable error.

as ΔS for vaporization of a liquid, and would forbid a useful estimation of reaction entropy. This condition may not affect all solutes; the computed gas phase spectrum of ((−)-sparteine)$PdCl_2$, for example, has no modes below 80 cm^{-1}. If the evaluation of a solute's internal and external entropy components by QM and MD, respectively, can be validated, this approach would allow the calculation of free energy changes, but not total enthalpy and entropy changes separately.

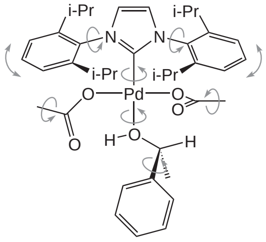

ν (cm^{-1})	S (cal/mol·K)	ν	S
6.6	8.8	35.8	5.5
11.8	7.7	38.7	5.3
15.5	7.1	41.0	5.2
19.7	6.7	43.3	5.1
25.7	6.1	45.8	5.0
33.9	5.6	47.3	4.9

Figure 5.4: Example of low frequency vibrational modes calculated in vacuum and their contribution to internal entropy ($S = \frac{u}{e^u - 1} - ln(1 - e^u), u = \frac{h\nu}{kT}$).

To avoid the polarizable continuum method, cycle II in Figure 5.3 uses MD to compute the interaction energy of solute and solvent, as well as the dynamic properties of the (again rigid) solute and solvent. Enthalpy and entropy of the solute's internal modes, along with the solute's electronic energy, would be provided by QM. To describe the desolvation of solutes, the forcefield employed must be capable of allowing the charge distributions of species to respond to their environments. In this formulation, total entropy and enthalpy changes would be accessible, but the inaccuracies of treating low-frequency vibrational modes as solvent-independent would persist. Also, sampling enough configuration-space to converge the entropy of the entire solute-solvent system may prove intractable.

Cycle III provides a homogeneous treatment of all the dynamic properties of the solute-solvent system by entrusting them to unconstrained MD and taking only the electronic energy change between the reactants and products in their minimum-energy geometries from QM. This scheme would require a forcefield capable of describing the polarizability and vibrational properties of catalytic species, and in turn would allow solutes with loose degrees of freedom to respond to the solvent environment. Transition states would pose difficulties in this scheme, and activation barriers may best be treated with a purely QM scheme and grafted onto an MD-derived energy profile.

The elements of these schemes, and possible variations on them, are plausible but not yet proved, and are meant to highlight means by which we might expand our abilities. Two more obvious areas for improvement are speed and accuracy in evaluating electronic energies, and the attention of many is focused on each. The B3LYP functional was shown to reproduce atomization[6] energies of small molecules with an average absolute deviation of 3.11 kcal/mol[101] using a large basis set (6-311+G(3df,2p)[102]). This permits useful thermochemical investigations, but more sophisticated (time consuming) techniques (configuration interaction, time-dependent density functional theory) are required to capture, for example, the splitting of spin states of metals in symmetric environments or excited state energies. New density functionals have been developed for specific applications such as activation energies[103, 104] and van der Waals interactions[20]. New families of functionals incorporating two-electron in addition to one-electron properties[105] may take another step forward in accuracy. Quantum Monte Carlo techniques, though presently handicapped by computer speeds, will place arbitrarily small error bars around the electronic energy within the Born-Oppenheimer approximation.

More so than accuracy, a premium is placed on speed here, because of the belief that today when a model fails to represent reality, it is more often because the contents of the model are incorrect or incomplete than because the physics within the model is inaccurately quantified. For examples, models are often scaled down from real systems by omitting atoms thought to be superfluous, or they belong to an incorrect mechanistic pathway, or they are treated as gas phase or zero-Kelvin when solvation or temperature effects are important. Computer architectures will continue to evolve, but acceleration also comes from new algorithms and a knowledge of what physical phenomena can be roughly approximated during a simulation while still obtaining the desired quantity with accuracy. Linear scaling techniques[106] that take advantage of the low overlap between distant electrons in a system are allowing large models to be treated with a uniform level of quantum mechanics (even including dynamics) instead of resorting to a mixed QM/MD scheme. In another

---

[6] Note that atomization energies provide a stiffer test of accuracy than reaction energies in which bonding is largely conserved.

example, the excited state dynamics of fluorene oligomers were followed by combining an ab initio time-dependent Hartree-Fock approach to calculate energies on the excited potential surface with a fast empirical INDO (intermediate neglect of differential overlap) scheme for obtaining Hamiltonian elements[107]. More all-atom simulations, performed with larger basis sets, would avoid many of the pitfalls mentioned in this chapter which are found to underpin models' inaccuracies.

Other tools under development that will aid theoretical investigations of real catalysts include the ab initio production of spectroscopic properties. As calculated NMR shifts become accurate and routine for relevant nuclei they will aid in determining the structure of new active species[7]. An important discovery in the field of hydrodesulfurization was a unique Mössbauer signal from Co/MoS_2 samples of different composition which correlated more closely with catalytic activity than did other (small molecule adsorption, x-ray) measurements[108]. The signal itself, however, did not offer a geometric interpretation and the atomic-scale features of HDS active sites remained unknown. Modeling the thermodynamic stability and Mössbauer spectra[109] of structures proposed in the literature may allow the identification of the true active site.

As the speed of calculations allows a higher throughput of jobs (be they possible intermediates in proposed mechanisms or variations on a new catalyst design), more human time is required to construct and vary molecular structures for input files and create initial guesses for transition state geometries. Automating these tasks, already underway in some software packages, will be necessary to apply new computer power to large screening efforts without wasting man-hours on menial work. For now, molecules to be studied are unique enough to be built on a case-by-case basis and calculations last long enough that this is not a bottleneck to progress.

5.3 Introduction Redux

Theoretical investigations into catalytic cycles have fallen short of tangible progress measured in new reactions or more atom efficient, energy efficient, or environmentally friendly versions of known reactions. In terms of the progression in Figure 1.1, most efforts fail to leave the computational

---

[7] And help determine the structure of metal-ligand complexes when NMR spectra show the desired complex did not form.

stages. In my limited experience, theorists have become proficient in obtaining new insights into existing reactions but have not reached the final goal of designing and correctly predicting the properties of a functioning new catalyst. The fact that understanding which had not been gained through complimentary techniques is consistently achieved testifies to the development of methods for the fast and accurate evaluation of the total energy of finite and periodic systems. There are natural reasons for progress to dwindle after this point though. Theory groups are often not in a close collaboration with an experimental group which can act on new designs that might be suggested. In this case the modelers may see their responsibility as ending with the publication of their results. In other cases (whether due to the unlimited flexibility of 'constructing' molecules in a computer or their ignorance of plausible syntheses) theorists have suggested catalysts which have proven thermodynamically unstable or outside the reach of known syntheses. Even a design predicted to behave favorably in the reaction of interest may fail in the experimental testing because of a side reaction not considered in the computational screening. If the scheme proposed in Figure 5.5 is to become routine it is in the interests of theorists to generate confidence among possible experimental collaborators by carefully screening their suggestions for stability and poisoning.

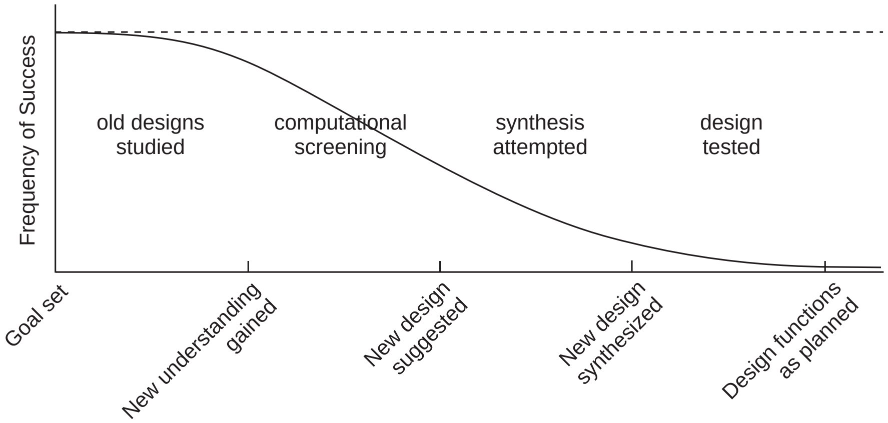

Figure 5.5: Progress in modeling studies of catalysis, and the author's estimate of success rates.

However, the technical deficiencies discussed in the previous section and difficulties forseeing modes of catalyst deactivation are not alone responsible for the lack of computationally designed catalysts. Too many modeling campaigns are *intended* to conclude with new understanding of a reaction. Perhaps because results can be published at this point, or perhaps because of the risk of investing further effort, most investigations are limited to reactions which have already been experimentally demonstrated. If the accuracy of computational methods has truly matured to a predictive power, then we should concern ourselves as much with modeling as-yet-unknown reactions as with dissecting proven ones. Developing computational assays does take more time than applying them, but judging by current literature the overwhelming majority of computation is applied to preexisting reactions.

Figure 5.6 illustrates a complimentary role of simulations in catalysis in terms of a putt-putt golf hole in which the ball is putted into the mouth of an unseen network of tunnels. After navigating the series of junctions, the ball emerges from one of many outlets directed either toward or away from the final goal. Putting into the network is like testing a given catalyst formulation under some conditions: one experiment reveals whether the ‘decisions’ made by the catalyst in situ led to the desired reaction or one of many possible failures. The single experiment does not explain why a particular path was taken at each junction nor offer information regarding the junctions left unsampled. Calculations can be brought to bear on a particular junction (whether or not it is heavily sampled in situ) by considering reaction channels (transition states) leading away from a proposed intermediate. Used skillfully and corroborated with real observations, models can suggest what variables must be optimized to tune a catalytic cycle’s free energy surface toward the desired reactivity. *De novo* prediction of a catalyst’s behavior would require (correctly) modeling *every* step[8] in a network, and this is now unrealistic. Determining the qualitative result of a new reaction is still best left to Mother Nature, who works efficiently in parallel and determines the flux of reactant through every step in a reaction network correctly by definition.

This discussion neglects the powerful experimental techniques developed for probing the same hidden workings of catalytic cycles. These methods can be more direct (in situ spectroscopic and kinetic measurements study real species while calculations address models) or less direct (studies of metal-carbonyl stretching frequencies and crystallography lead to *inferences* about actual transition

---

[8] Even unforeseen steps

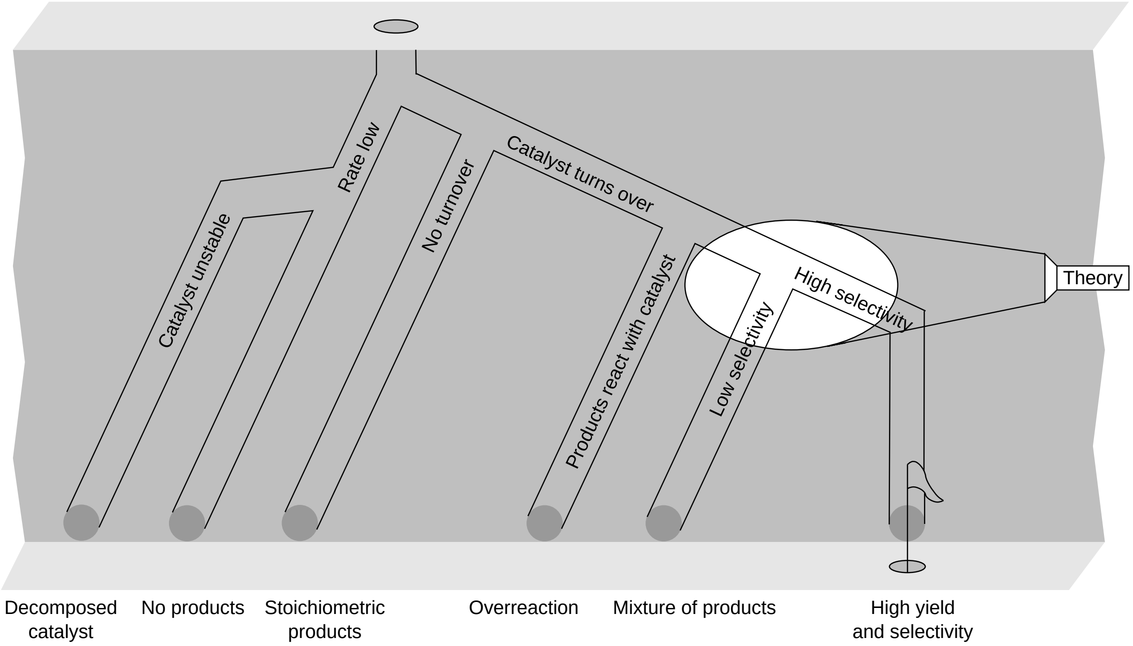

Figure 5.6: Complimentary roles of simulation and experiment in catalysis.

states) than simulations. Computation may be cheaper than many experimental techniques, but it is still often slower and its speed and applicability are unfortunately tied to the size of the catalyst.

High-throughput combinatorial strategies have been cited as the opposite approach to catalyst discovery. Also a maturing field, this technique has already produced success stories ([110] and references within), and does not require prior mechanistic studies like a computational campaign. Application of high-throughput technology requires catalysts whose synthesis can be automated (natural for heterogeneous studies) or large prefabricated ligand libraries. Evaluations of catalyst performance must also be mechanized, which allows success and failure to be measured without an understanding of why a given formulation succeeded or failed. This kind of understanding is intrinsic in a computational scheme that screens for stability, activity and selectivity explicitly. Recall that these separate properties of a catalyst could be traced back to modifications of the bispidine framework in Chapter 3. Knowledge of such relationships recognizes the potential strengths of a candidate which would fail in both experimental and virtual screens, and allows that candidate to be reposited in an intelligently evolved form. It will not be surprising for collaborations between the two complimentary strategies[111] to become more popular.

I suggest asymmetric catalysis is a subdiscipline in which computation may begin to lead to new catalysts. Screens in this arena take advantage of theory's proven ability to predict activation barriers and slight energy differences between isomeric transition states (whether they are caused by electrostatics, sterics, solvation, bond strain, etc.) An integrated experimental/theoretical protocol, which could be implemented in routinely equipped laboratories, might involve experimentally screening potential candidates which were widely separated in parameter-space. The object of this screen would not be to identify a highly active and selective catalyst in the first iteration, but to determine the qualitative behavior (as in Figure 5.6) of a variety of archtypes. If this screen identified a candidate which was capable of shuttling the substrate through all or most of a catalytic cycle with no selectivity, simulations could be employed to identify the minor adjustments in parameter-space (the design of stereogenic 'side-chains') necessary for tuning in stereoselective thermodynamics. This collaboration would avoid a weakness of theory (trying to design a working cycle from scratch) *and* of experiments (the repetitive synthesis of stereoactive organic ligands whose slight geometric differences lead to changes in reactivity which are unpredictable by inspection).

What this thesis demonstrates is the ability of computational tools to uncover the causes of observed reactivity which had been inaccessible by complimentary methods. The theoretical description of transition states and how they depend on chemical composition and solvent has proven qualitatively and quantitatively illuminating. By comparing experimental and calculated data, proposed mechanisms can be validated and discredited. Algorithms for the computational screening of new catalysts can be developed and used to intelligently evolve catalyst properties.

If the application of such screens in Chapters 3 and 4 has so far only produced "10,000 ways that won't work," it is difficult to interpret. Perhaps one of the variations on the N-heterocyclic carbene framework already tested would yield a stable, selective catalyst, or perhaps all the candidates would suffer from a concurrent, unselective reaction. In either case, Edison's optimism ("I am not discouraged, because every wrong attempt discarded is another step forward.") appears more affordable *after* outright success.

Bibliography

[1] K. Sabbagh. *21st-Century Jet.* Scribner, New York, 1996.

[2] J. Tersoff. *Phys. Rev. B*, 38:9902, 1988.

[3] D. W. Brenner. *Phys. Rev. B*, 42:9458, 1990.

[4] A. C. T. van Duin, S. Dasgupta, F. Lorant, and W. A. Goddard III. *J. Phys. Chem. A*, 105:9396, 2001.

[5] A. C. T. van Duin, A. Strachan, S. Stewman, Q. Zhang, X. Xu, and W. A. Goddard III. *J. Phys. Chem. A*, 107:3803, 2003.

[6] A. Strachan, A. C. T. van Duin, D. Chakraborty, S. Dasgupta, and W. A. Goddard III. *Phys. Rev. Lett.*, 91:9301, 2003.

[7] Q. Zhang. *Atomistic simulations of barium titanate.* PhD thesis, California Institute of Technology, 2004.

[8] W. A. Goddard III, Q. Zhang, M. Uludogan, A. Strachan, and T. Cagin. The ReaxFF polarizable reactive force fields for molecular dynamics simulation of ferroelectrics. R. E. Cohen, editor, *Fundamental Physics of Ferroelectrics.* 2002.

[9] T. Vreven and K. Morokuma. *J. Comp. Chem.*, 21(16):1419–1432, 2000.

[10] T. Vreven, B. Mennucci, C. O. da Silva, K. Morokuma, and J. Tomasi. *J. Chem. Phys.*, 115(1):62–72, 2001.

[11] R. B. Murphy, D. M. Philipp, and R. A. Friesner. *J. Comp. Chem.*, 21(16):1442–1457, 2000.

[12] U. Richter and M. Krauss. *J. Am. Chem. Soc.*, 123:6973–6982, 2001.

[13] P. N. Day, J. H. Jensen, M. S. Gordon, S. P. Webb, W. J. Stevens, M. Krauss, D. Garmer, H. Basch, and D. Cohen. *J. Chem. Phys.*, 105(5):1968–1986, 1996.

[14] A. Szabo and N. S. Ostlund. *Modern Quantum Chemistry.* Dover Publications, Inc., 1996.

[15] Robert G. Parr and Weitao Yang. *Density-functional theory of atoms and molecules.* Oxford University Press, 1989.

[16] Wolfram Koch and Max C. Holthausen. *A Chemist's Guide to Density Functional Theory.* Wiley-VCH, 2001.

[17] Axel D. Becke. *J. Chem. Phys.*, 98(7):5648–5652, 1993.

[18] Chengteh Lee, Weitao Yang, and Robert G. Parr. *Phys. Rev. B*, 37(2):785–789, 1988.

[19] R. Colle and D. Salvetti. *Theor. Chim. Acta*, 37:329, 1975.

[20] Xin Xu and William A. Goddard III. *PNAS*, 101(9):2673–2677, 2004.

[21] R. S. Mulliken. *J. Chem. Phys.*, 23(10):1833–1840, 1955.

[22] W. J. Hehre, R. Ditchfield, and J. A. Pople. *J. Chem. Phys.*, 56(5):2257–2261, 1972.

[23] Michelle M. Francl, William J. Pietro, Warren J. Hehre, J. Stephen Binkley, Mark S. Gordon, Douglas J. DeFrees, and John A. Pople. *J. Chem. Phys.*, 77(7):3654–3665, 1982.

[24] P. C. Hariharan and J. A. Pople. *Theor. Chim. Acta.*, 28:213, 1973.

[25] P. Jeffrey Hay and Willard R. Wadt. *J. Chem. Phys.*, 82(1):299–310, 1985.

[26] D. D. Wagman, W. H. Evans, V. B. Parker, R. H. Schumm, I. Halow, S. M. Bailey, K. L. Churney, and R. L. Nutall. The NBS tables of chemical thermodynamic properties. *Journal of Physical and Chemical Reference Data*, 11(Suppl. 2), 1982.

[27] P. J. Linstrom and W. G. Mallard, editors. *NIST Chemistry WebBook, NIST Standard Reference Database Number 69.* National Institute of Standards and Technology, Gaithersburg MD, 20899, March 2003. http://webbook.nist.gov.

[28] Takahiro Nishimura, Tomoaki Onoue, Kouichi Ohe, and Sakae Uemura. *J. Org. Chem.*, 64:6750–6755, 1999.

[29] Gerd-Jan ten Brink, Isabel W. C. E. Arends, and Roger A. Sheldon. *Science*, 287:1636–1639, 2000.

[30] Bradley A. Steinhoff and Shannon S. Stahl. *Organic Letters*, 4(23):4179–4181, 2002.

[31] E. M. Ferreira and B. M. Stoltz. *J. Am. Chem. Soc.*, 123:7725–7726, 2001.

[32] David R. Jensen, Jacob S. Pugsley, and Matthew S. Sigman. *J. Am. Chem. Soc.*, 123:7475–7476, 2001.

[33] Karl P. Peterson and Richard C. Larock. *J. Org. Chem.*, 63:3185–3189, 1998.

[34] Bradley A. Steinhoff, Shannon R. Fix, and Shannon S. Stahl. *J. Am. Chem. Soc.*, 124(5):766–767, 2002.

[35] Jaime A. Mueller, Christopher P. Goller, and Matthew S. Sigman. *J. Am. Chem. Soc.*, 126:9724–9734, 2004.

[36] Daniel D. Caspi, David C. Ebner, Jeffrey T. Bagdanoff, and Brian M. Stoltz. *Adv. Synth. Catal.*, 346:185–189, 2004.

[37] Iliyas Sayyed Ali and Arumugam Sudalai. *Tetrahedron Letters*, 43:5435–5436, 2002.

[38] Jaime A. Mueller and Matthew S. Sigman. *J. Am. Chem. Soc.*, 125(23):7005–7013, 2003.

[39] J. T. Bagdanoff, E. M. Ferreira, and B. M. Stoltz. *Organic Letters*, 5(6):835–837, 2003.

[40] Jeffrey T. Bagdanoff and Brian M. Stoltz. *Angew. Chem., Int. Ed.*, 43:353–357, 2004.

[41] Willard R. Wadt and P. Jeffrey Hay. *J. Chem. Phys.*, 82(1):284–298, 1985.

[42] A. Höllwarth, M. Böhme, S. Dapprich, A. W. Ehlers, A. Gobbi, V. Jonas, K. F. Köhler, R. Stegmann, A. Veldkamp, and G. Frenking. *Chem. Phys. Lett.*, 208:237, 1993.

[43] Jaguar 5.0, Schrödinger, L.L.C., Portland, OR, 1991-2003.

[44] Masashi Yamakawa, Hisashi Ito, and Ryoji Noyori. *J. Am. Chem. Soc.*, 122:1466–1478, 2000.

[45] Shohei Hashiguchi, Akio Fujii, Jun Takehara, Takao Ikariya, and Ryoji Noyori. *J. Am. Chem. Soc.*, 117(28):7562–7563, 1995.

[46] Raissa M. Trend and Brian M. Stoltz. *J. Am. Chem. Soc.*, 126:4482–4483, 2004.

[47] Michael L. Steigerwald and William A. Goddard III. *J. Am. Chem. Soc.*, 106:308–311, 1984.

[48] Takahiro Hosokawa and Shun-Ichi Murahashi. *Acc. Chem. Res.*, 23:49–54, 1990.

[49] Jason M. Keith, Robert J. Nielsen, Jonas Oxgaard, and William A. Goddard III. *J. Am. Chem. Soc.*, accepted, 2005.

[50] Shannon S. Stahl, Joseph L. Thorman, Ryan C. Nelson, and Michael A. Kozee. *J. Am. Chem. Soc.*, 123:7188–7189, 2001.

[51] Clark R. Landis, Christine M. Morales, and Shannon S. Stahl. *J. Am. Chem. Soc.*, 126(50):16302–16303, 2004.

[52] Jaime A. Mueller, David R. Jensen, and Matthew S. Sigman. *J. Am. Chem. Soc.*, 124(28):8202–8203, 2002.

[53] David R. Jensen and Matthew S. Sigman. *Organic Letters*, 5(1):63–65, 2003.

[54] Per-Ola Norrby, Torben Rasmussen, Jan Haller, Thomas Strassner, and K. N. Houk. *J. Am. Chem. Soc.*, 121:10186–10192, 1999.

[55] Kenneth B. Wiberg and William F. Bailey. *J. Am. Chem. Soc.*, 123:8231–8238, 2001.

[56] Tao Ke, Charles R. Wescott, and Alexander M. Klibanov. *J. Am. Chem. Soc.*, 118:3366–3374, 1996.

[57] Kenny B. Lipkowitz and Marisa C. Kozlowski. *Synlett*, (10):1547–1565, 2003.

[58] T. Ebner, M. Eichelbaum, P. Fischer, and C. O. Meese. *Ach. Pharm. (Weinheim)*, 322:399, 1989.

[59] Brenton T. Smith, John A. Wendt, and Jeffrey Aubé. *Org. Lett.*, 4(15):2577–2579, 2002.

[60] Donald J. Gallagher, Shengde Wu, Nikola A. Nikolic, and Peter Beak. *J. Org. Chem.*, 60:8148–8154, 1995.

[61] Michael J. Dearden, Catherine R. Firkin, Jean-Paul R. Hermet, and Peter O'Brien. *J. Am. Chem. Soc.*, 124:11870–11871, 2002.

[62] H. Lecoq. *Bull. Soc. Chim. Fr.*, page 153, 1943.

[63] A. El-Shazly, T. Sarg, A. Ateya, E. A. Aziz, L. Witte, and M. Wink. *Pharmazie*, 51:768, 1996.

[64] D. St. C. Black, G. B. Deacon, and M. Rose. *Tetrahedron*, 51(7):2055–2076, 1995.

[65] Adolf Gogoll, Charlotte Johansson, Andreas Axén, and Helena Grennberg. *Chem. Eur. J.*, 7(2):396–403, 2001.

[66] G.-Jan ten Brink, I. W. C. E. Arends, M. Hoogenraad, Göran Verspui, and R. A. Sheldon. *Adv. Synth. Catal.*, 345(4):497–505, 2003.

[67] Kristina Hallman, Anders Frölander, Tebikie Wondimagegn, Mats Svensson, and Christina Moberg. *PNAS*, 101(15):5400–5404, 2004.

[68] T. F. Blackburn and J. Schwartz. *J. Chem. Soc., Chem. Comm.*, 157–158, 1977.

[69] Mitchell J. Schultz, Candice C. Park, and Matthew S. Sigman. *Chem. Comm.*, 3034–3035, 2002.

[70] Sari Paavola, Krister Zetterberg, Timofei Privalov, Ingeborg Csöregh, and Christina Moberg. *Adv. Synth. Catal.*, 346:237–244, 2004.

[71] Kristina Hallman and Christina Moberg. *Adv. Synth. Catal.*, 343(3):260–263, 2001.

[72] David R. Jensen, Mitchell J. Schultz, Jaime A. Mueller, and Matthew S. Sigman. *Angew. Chem. Int. Ed.*, 42:3810–3813, 2003.

[73] Alexandre Alexakis, Caroline L. Winn, Frederic Guillen, Julien Pytkowicz, Sylvain Roland, and Pierre Mangeney. *Adv. Synth. Catal.*, 345(3):345–348, 2003.

[74] Sylvain Roland, Max Audouin, and Pierre Mangeney. *Organometallics*, 23:3075–3078, 2004.

[75] D. Enders, H. Gielen, and K. Breuer. *Tetrahedron: Asymmetry*, 8(21):3571–3574, 1997.

[76] Mark T. Powell, Duen-Ren Hou, Marc C. Perry, Xiuhua Cui, and Kevin Burgess. *J. Am. Chem. Soc*, 123:8878–8879, 2001.

[77] Gerd-Jan ten Brink, Isabel W. C. E. Arends, and Roger A. Sheldon. *Adv. Synth. Catal.*, 344:355–369, 2002.

[78] Bradley A. Steinhoff, Ilia A. Guzei, and Shannon S. Stahl. *J. Am. Chem. Soc.*, 126:11268–11278, 2004.

[79] Yukio Fujii, Hiromichi Yamada, and Masateru Mizuta. *J. Phys. Chem.*, 92:6768–6772, 1988.

[80] Sherril D. Christian, Harold E. Affsprung, and James R. Johnson. *J. Chem. Soc.*, page 1896, 1963.

[81] W. L. Masterton and M. C. Gendrano. *J. Phys. Chem.*, 70(9):2895, 1966.

[82] Michael M. Konnick, Ilia A. Guzei, and Shannon S. Stahl. *J. Am. Chem. Soc.*, 126:10212–10213, 2004.

[83] Rex T. Skodje and Donald G. Truhlar. *J. Phys. Chem.*, 85:624–628, 1981.

[84] E. F. Breheret and M. M. Martin. *J. Lumin.*, 17:49, 1978.

[85] Frederic Guillen, Caroline L. Winn, and Alexandre Alexakis. *Tetrahedron: Asymmetry*, 12:2083–2086, 2001.

[86] Andrew W. Waltman and Robert H. Grubbs. *Organometallics*, 23:3105–3107, 2004.

[87] Vincent Cesar, Stephane Bellemin-Laponnaz, and Lutz H. Gade. *Organometallics*, 21:5204–5208, 2002.

[88] J. Kua and W. A. Goddard III. *J. Phys. Chem. B*, 102:9481–9491, 1998.

[89] D. E. Woon and Jr. T. H. Dunning. *J. Chem. Phys.*, 98:1358, 1993.

[90] Jan M. L. Martin. *J. Chem. Phys.*, 108:2791, 1998.

[91] Karsten Reuter, Daan Frenkel, and Matthias Scheffler. *Phys. Rev. Lett.*, 93(11):116105, 2004.

[92] R. A. Periana, D. J. Taube, S. Gamble, H. Taube, T. Satoh, and H. Fujii. *Science*, 280:560–564, 1998.

[93] J.S. Casas, A. Castineiras, Y. Parajo, M.L. Perez-Paralle, A. Sanchez, A. Sanchez-Gonzalez, and J. Sordo. *Polyhedron*, 22:1113–1121, 2003.

[94] M. C. Payne, M. P. Teter, D. C. Allan, T. A. Arias, and J. D. Joannopoulos. *Rev. Mod. Phys*, 64:1045, 1992.

[95] A. F. Wells. *Structural Inorganic Chemistry.* Clarendon Press, Oxford, fourth edition, 1975.

[96] Peter Atkins. *Physical Chemistry.* Freeman, sixth edition, 1998.

[97] D.J. Tannor, B. Marten, R. Murphy, R.A. Friesner, D. Sitkoff, A. Nicholls, M. Ringnalda, W.A. Goddard III, and B. Honig. *J. Am. Chem. Soc.*, 116:11875, 1994.

[98] Chistopher J. Cramer and Donald G. Truhlar. *Chem. Rev.*, 99:2161–2200, 1999.

[99] Christine Peter, Chris Oostenbrink, Arthur van Dorp, and Wilfred F. van Gunsteren. *J. Chem. Phys.*, 120(6):2652–2661, 2004.

[100] Shiang-Tai Lin, Mario Blanco, and William A. Goddard III. *J. Chem. Phys.*, 119(22):11792–11805, 2003.

[101] Larry A. Curtiss, Krishnan Raghavachari, Paul C. Redfern, and John A. Pople. *J. Chem. Phys.*, 106(3):1063–1079, 1997.

[102] Michael J. Frisch, John A. Pople, and J. Stephen Binkley. *J. Chem. Phys.*, 80(7):3265–3269, 1984.

[103] Benjamin J. Lynch, Patton L. Fast, Maegan Harris, and Donald G. Truhlar. *J. Phys. Chem. A*, 104(21):4811–4815, 2000.

[104] Jeung Ku Kang and Charles B. Musgrave. *J. Chem. Phys.*, 115(24):11040–11051, 2001.

[105] P. M. W. Gill, A. M. Lee, N. Nair, and R. D. Adamson. *J. Mol. Struct. (Theochem)*, 506:303–312, 2000.

[106] Anders M. N. Niklasson, C. J. Tymczak, and Matt Challacombe. *J. Chem. Phys.*, 118(19):8611–8620, 2003.

[107] Ignacio Franco and Sergei Tretiak. *J. Am. Chem. Soc.*, 126:12130–12140, 2004.

[108] H. Topsøe and B. Clausen. *Appl. Catal.*, 25:273, 1986.

[109] Yong Zhang, Junhong Mao, and Eric Oldfield. *J. Am. Chem. Soc.*, 124:7829–7839, 2002.

[110] Vince Murphy, Anthony F. Volpe Jr., and W. Henry Weinberg. *Current Opinion in Chemical Biology*, 7:427–433, 2003.

[111] Peter Strasser, Qun Fan, Martin Devenney, and W. Henry Weinberg. *J. Phys. Chem. B*, 107:11013–11021, 2003.